Journal of Statistical Mechanics: Theory and Experiment
An IOP and SISSA journal

Maximum valency lattice gas models

Srikanth Sastry[1], Emilia La Nave[2] and Francesco Sciortino[2]

[1] Jawaharlal Nehru Centre for Advanced Scientific Research, Jakkur Campus, Bangalore 560064, India
[2] Dipartimento di Fisica and INFM-CNR-SOFT, Università di Roma La Sapienza, P.le A. Moro 2, I-00185 Rome, Italy
E-mail: sastry@jncasr.ac.in, emilia.lanave@phys.uniroma1.it and francesco.sciortino@phys.uniroma1.it

Received 15 September 2006
Accepted 21 November 2006
Published 11 December 2006

Online at stacks.iop.org/JSTAT/2006/P12010
doi:10.1088/1742-5468/2006/12/P12010

Abstract. We study lattice gas models with the imposition of a constraint on the maximum number of bonds (nearest-neighbour interactions) that particles can participate in. The critical parameters, as well as the coexistence region, are studied using the mean field approximation and the Bethe–Peierls approximation. We find that the reduction of the number of interactions suppresses the temperature–density region where the liquid and gas phases coexist. We confirm these results from simulations using the histogram reweighting method employing grand canonical Monte Carlo simulations.

Keywords: classical phase transitions (theory), structural colloidal and polymer glasses (theory), colloids, slow relaxation and glassy dynamics

ArXiv ePrint: cond-mat/0609388

J. Stat. Mech. (2006) P12010

1742-5468/06/P12010+11$30.00

Contents

1. Introduction

The study of the gel state of matter in colloidal systems is receiving significant attention in recent years [1]–[4]. At the heart of this interest lies the hope that these studies will help in understanding differences and similarities in the processes of formation of arrested states of matter at low packing fraction ϕ and, in particular, the inter-relations between gels and glasses. A similarly ambitious additional goal is to provide a new route for understanding the intrinsic properties of the process of formation of physical gels in systems more complicated than colloids, such as gels formed by reversible cross-linking of polymeric chains [5] and gelation in protein solutions [6]. The full comprehension of both these aggregation processes are of extreme importance in the food industry, in the protein crystallization process and in the design of novel biomaterials [7].

One of the key questions of interest concerns the interplay between the process of formation of a long-living network and the process of phase separation into colloid-rich and colloid-poor regions [8]–[12]. Indeed, the increase of the bond interaction strength (relative to the thermal energy) controls both the increase of the inter-particle bond lifetime (and as a consequence the lifetime of the spanning network) and the increase of the driving force of formation of locally dense packed states, which progressively favour nucleation of the 'liquid' (colloid-rich) phase [4]. As a result, the establishment of conditions such that a connected percolating structure able to sustain stress survives for times longer than the observation time is often preempted by phase separation. For spherical attractive interaction potentials, it has been found that phase separation is always dominant at low densities and arrested states at low packing fractions ϕ can be reached only in a non-homogeneous state, whose morphology is determined by the phase separation process [13]–[19].

A possible mechanism to generate arrested states of low packing fraction in the absence of phase separation has been recently proposed and supported by off-lattice simulations [20, 21]. It has been shown that the region in the T–ϕ plane in which a two-phase coexistence is thermodynamically preferred as compared to the homogeneous fluid state can be progressively reduced (both in T and ϕ) by decreasing the maximum number

doi:10.1088/1742-5468/2006/12/P12010

J. Stat. Mech. (2006) P12010

of possible pairwise bonded interactions. In an equivalent language, the reduction—at fixed interaction potential range—of the colloid surface allowing for inter-particle bonding progressively suppresses phase separation [22, 23]. According to these ideas, colloidal particles with a limited number of attractive spots are the best candidates for gel formation. Interestingly enough, these ideas also carry over to the case of protein solutions, where the character of the amino acids on the surface of the protein controls the strength and the directionality of the inter-protein interaction [6].

In this paper, we present a lattice gas model, which we solve in the Bragg–Williams mean field approximation and in the Bethe–Peierls quasi-chemical approximation, and which allows us to visualize in a clear way the relation between the limitation of the maximum number of interactions and the amplitude of the phase-separated region in the T–ϕ phase diagram. We complement these calculations with Monte Carlo simulations of the liquid–gas phase coexistence, to assess the reliability of the mean field solutions. The reported results confirm that the reduction of the maximum number of interactions is indeed an efficient mechanism for generating thermodynamically stable states at extremely low temperatures.

2. The model

The system we consider is a nearest-neighbour lattice gas, with occupancy variables n_i at each node of a lattice with γ nearest-neighbour sites.

The Hamiltonian for the system is written in the usual form, with the occupancy variables n_i that can take values 0 or 1, and ϵ being the interaction strength, as

$$H = -\epsilon \sum_{\langle ij \rangle}^{*} n_i n_j \tag{1}$$

but with the * indicating that the sum is only over such bond configurations that have, at each vertex, a maximum of γ_{m} bonds, although there is no restriction on the number of nearest-neighbour occupied sites which can have any value from 0 to γ. In other words, a 'bond' exists between a pair of occupied neighbours i and j, and correspondingly an interaction energy of $-\epsilon$ is counted for if and only if neither i nor j has greater than γ_{m} bonds, including the ij bond.

For concreteness, in the following, we consider the lattice on which the Hamiltonian above is defined to be the FCC lattice, with $\gamma = 12$. The interaction strength $\epsilon = 1$ is shown in all calculations.

For the purposes of mean field theory, we can write this as

$$H = -\frac{\epsilon}{2} \sum_i n_i f\left(\sum_j^{\gamma} n_j \right) \tag{2}$$

where the first sum i runs over all lattice sites, and the second sum j runs over all γ nearest neighbours of site i, and with

$$f(x) = x, \qquad x \leq \gamma_{\mathrm{m}} \tag{3}$$

$$= \gamma_{\mathrm{m}}, \qquad x > \gamma_{\mathrm{m}} \tag{4}$$

J. Stat. Mech. (2006) P12010

where γ_m denotes the maximum number of interactions, or valency, allowed for a particle at any site. When $\gamma_m = \gamma$, one recovers the simple lattice gas. In the following, we consider the behaviour of the system when the parameter γ_m is varied between the limits $\gamma_m = 0$ (when one has a non-interacting *paramagnetic* lattice gas) and $\gamma_m = \gamma$ (when one has the simple nearest-neighbour lattice gas). Note that the Hamiltonian defined in equation (1) is not the same in detail as that defined in equation (2). This can be most easily seen by considering, for example, a simple cubic lattice with $\gamma = 6$ and the maximum valency $\gamma_m = 3$. If one considers a configuration where a given site has all γ neighbouring sites occupied, and the neighbours have no other neighbouring sites occupied, the interaction energies as calculated from equation (1) and equation (2) differ. Nevertheless, we use equation (2) for the Bragg–Williams mean field approximation since in the mean field approximation they are equivalent, using the exact equation (1) for the Bethe–Peierls approximation and for the simulations.

3. Bragg–Williams mean field approximation

In order to perform the mean field calculation, we approximate the function f as

$$f(x) = \gamma_m \tanh(x/\gamma_m) \tag{5}$$

which has the desired linear behaviour for small x and a constant value of γ_m at large x. Further, the mean field approximation amounts to writing $\sum_j^{nn} n_j = \gamma\langle n\rangle$ where $\langle n\rangle$ is the average occupancy, given by $\langle n\rangle = \sum_i n_i/N$ where N is the total number of sites. With this approximation, the thermodynamic potential Ω in the grand canonical ensemble may be written as

$$\Omega/N = -\frac{\epsilon}{2}\gamma_m\langle n\rangle \tanh\left(\frac{\gamma\langle n\rangle}{\gamma_m}\right) - \mu\langle n\rangle + k_B T[\langle n\rangle \log\langle n\rangle + (1-\langle n\rangle)\log(1-\langle n\rangle)] \tag{6}$$

where μ is the chemical potential, T is the temperature, k_B is the Boltzmann constant and $\langle n\rangle$ is the occupancy, given μ and T, that minimizes Ω. Imposing the minimization condition,

$$\frac{\partial\Omega}{\partial\langle \mathbf{n}\rangle} = 0$$

allows one to eliminate μ and write the thermodynamic potential Ω in terms of T and $\langle n\rangle$. Further, since $\Omega = -PV = -PN$ (where P is the pressure, and the system volume for the lattice gas $V = N$ the number of sites) one obtains in this way the equation of state of the system:

$$P = -\frac{\epsilon}{2}\gamma\langle n\rangle^2 \operatorname{sech}^2\left(\frac{\gamma\langle n\rangle}{\gamma_m}\right) - k_B T \log(1-\langle n\rangle). \tag{7}$$

The condition for the critical point is given by

$$\frac{\partial P}{\partial\langle n\rangle} = 0$$

and

$$\frac{\partial^2 P}{\partial\langle n\rangle^2} = 0.$$

J. Stat. Mech. (2006) P12010

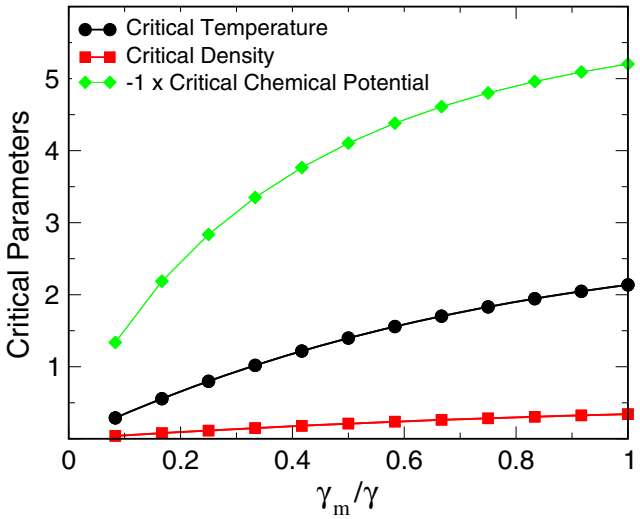

Figure 1. Critical density, critical temperature and chemical potential as a function of parameter $\gamma_{\rm m}$ for the Bragg–Williams mean field approximation.

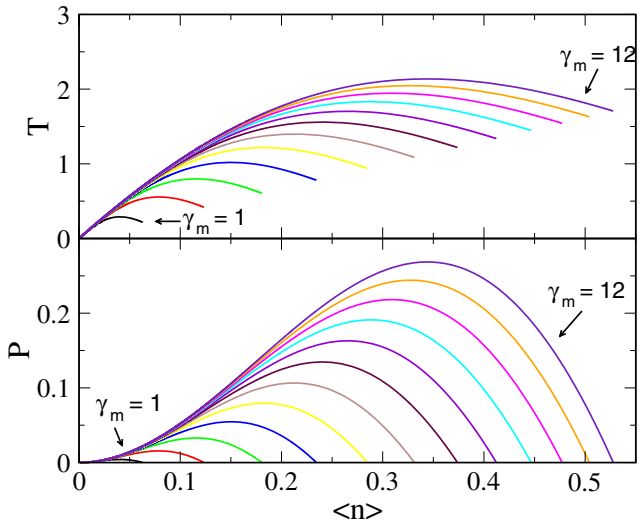

Figure 2. The mean field spinodals in the $(\langle n\rangle, T)$ plane (top panel) and in the $(\langle n\rangle, P)$ plane (lower panel) for different values of the parameter $\gamma_{\rm m}$. Calculated for $\gamma = 12$ and $\epsilon = 1$.

From these, one obtains the critical density and the critical temperature, which depend on the parameter $\gamma_{\rm m}/\gamma$ and are plotted in figure 1. From the figure, it is clear that both the critical density and the critical temperature go to zero as the variable $\gamma_{\rm m}/\gamma$ goes to zero.

We next calculate the spinodals that demarcate the region of instability in the $(\langle n\rangle, T)$ and in the $(\langle n\rangle, P)$ planes, which are shown in figure 2. Consistent with expectations based on the behaviour of the critical density and temperature, the region of instability also shrinks with the reduction in the valency.

4. Bethe–Peierls approximation

As an improvement over the mean field approximation, we next consider the Bethe–Peierls approximation, which in the case of the simple lattice gas is equivalent to the Bethe lattice. As in the standard treatment (see, e.g., [24]), we consider a 'centre' site, and its surrounding neighbours. We write the probability that the centre site is occupied, with n nearest neighbours also being occupied, as

$$P(1,n) = \frac{1}{q}\exp(\beta\mu)C_n^{\gamma}\exp(\beta\epsilon n)\exp(\beta\mu n)z^n \qquad n \leq \gamma_{\mathrm{m}} \tag{8}$$

$$= \frac{1}{q}\exp(\beta\mu)C_n^{\gamma}\exp(\beta\epsilon\gamma_{\mathrm{m}})\exp(\beta\mu n)z^n \qquad n > \gamma_{\mathrm{m}} \tag{9}$$

where $\beta \equiv 1/k_{\mathrm{B}}T$, q is the normalization, and z is introduced to account for the influence of the rest of the lattice. The rest of the terms explicitly account for the interactions and the chemical potential corresponding to the number of occupied sites present. Similarly, the probability that the centre site is not occupied, with n neighbours occupied, is

$$P(0,n) = \frac{1}{q}C_n^{\gamma}\exp(\beta\mu n)z^n. \tag{10}$$

The normalization factor q is given by the condition

$$\sum_{n=0}^{\gamma}[P(1,n) + P(0,n)] = 1. \tag{11}$$

The average occupancy number $\langle n_0\rangle$ for the centre site is the probability that the centre is occupied regardless of the occupancy of the surrounding sites, that is:

$$\langle n_0\rangle = \sum_{n=0}^{\gamma} P(1,n). \tag{12}$$

The average occupancy number $\langle n_e\rangle$ for a given neighbour site is given by

$$\langle n_e\rangle = \frac{1}{\gamma}\sum_{n=0}^{\gamma} n[P(1,n) + P(0,n)]. \tag{13}$$

The unknown parameter z is now determined by the condition that these two occupancy numbers, $\langle n_0\rangle$ and $\langle n_e\rangle$, are equal to each other. Defining a function

$$g(z,\mu,T) = \langle n_0\rangle - \langle n_e\rangle,$$

the solution is found by the condition $g(z,\mu,T) = 0$. Determining z in this way, and using the expression for $\langle n_0\rangle$ above, one obtains the probability of occupation as a function of T and μ. In addition, imposing the condition that the first and second derivatives of g also vanish yields the condition for the critical point, since this vanishing of the first and second derivatives marks the change from the high temperature regime where only one solution exists, to the presence of more than one solution at lower temperatures. In addition, the condition that the first derivative vanishes is used to locate the spinodal points. Figure 3 shows the dependence of the critical density, temperature and the chemical potential on the parameter γ_{m} which is varied in integer steps for $\gamma = 12$. The case of

J. Stat. Mech. (2006) P12010

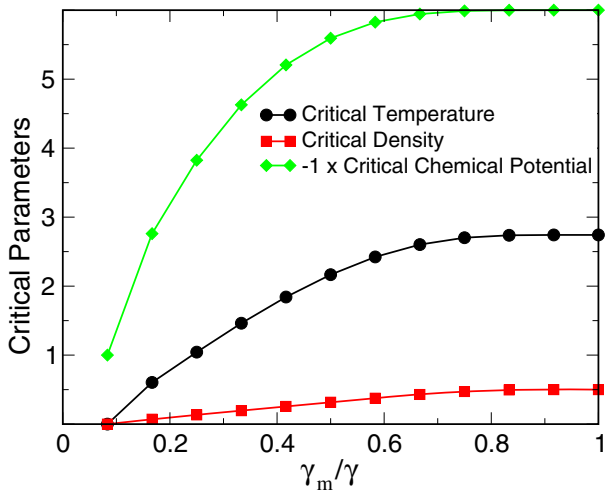

Figure 3. Critical density, critical temperature and chemical potential as a function of parameter γ_m for the Bethe–Peierls approximation.

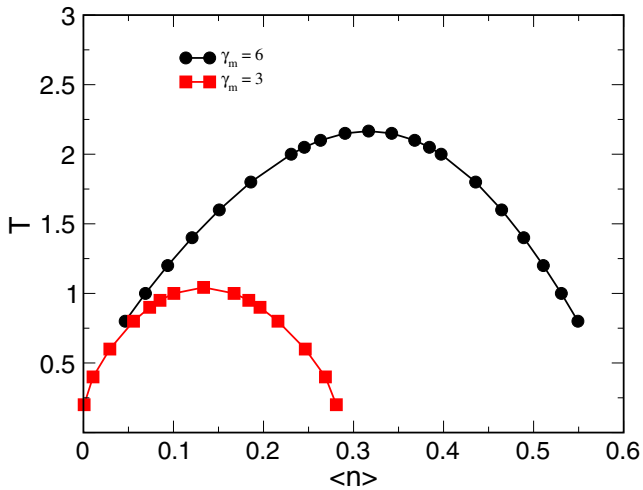

Figure 4. The Bethe–Peierls spinodal line evaluated for the specific cases of $\gamma = 12$ and $\gamma_m = 3, 6$.

$\gamma_m = \gamma$ reproduces the standard result for this approximation. It is seen that the critical temperature decreases very slowly at first as γ_m is reduced, but goes to zero for $\gamma_m = 1$.

We next calculate the spinodals that demarcate the region of instability in the $(\langle n \rangle, T)$ phase diagram for the cases $\gamma_m = 3, 6$, which are shown in figure 4. As in the mean field case the region of instability also shrinks with the reduction in the valency.

5. Simulations

In order to estimate the accuracy of the approximations above, we evaluate the critical parameters and the coexistence lines for different values of γ_m using computer simulations, employing the histogram reweighting technique [25]–[28]. In this method, histograms of

doi:10.1088/1742-5468/2006/12/P12010

J. Stat. Mech. (2006) P12010

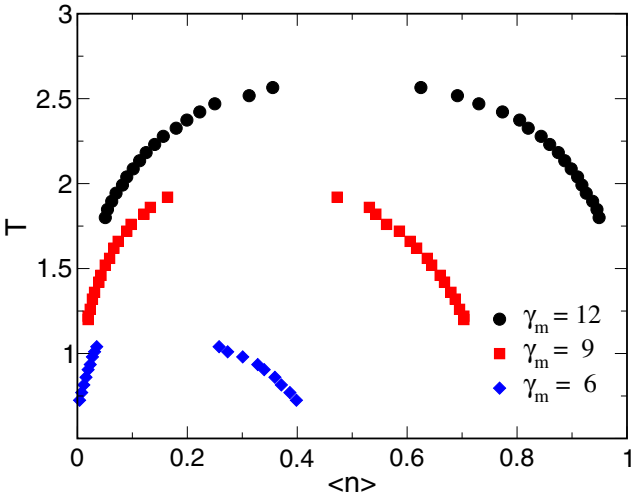

Figure 5. The coexistence curves for $\gamma_{\rm m} = 12, 9, 6$ from simulations, showing that the coexistence region shrinks as $\gamma_{\rm m}$ decreases.

sampled energies and number densities from simulations at different external parameters are used to estimate composite probability distributions, which in turn may be used to obtain information on phase equilibrium. To this end, we perform Monte Carlo simulations in the constant temperature and constant chemical potential ensemble for a lattice of 256 sites arranged in an FCC lattice. The energy of the system depends not only on which sites are occupied, but also which bonds exist in the system. Therefore, care must be taken that the formation and deletion of bonds obeys detailed balance. In the grand canonical simulations, it is sufficient, when a particle is inserted, to pick any of the possible bond configurations at random, with equal probability. At each simulated temperature and chemical potential, runs of length 2.5 million Monte Carlo cycles (MCS) are performed. The energies and number of particles every 100 MCS, after an equilibration of 0.5 million MCS, are used to build histograms $f_i(N, E)$ (where N is the number of particles and E is the energy), where $i = 1 \ldots R$ indexes the different runs at different μ and T values. As described in [26, 28], the composite probability distribution $\Gamma(N, E, \mu, \beta)$ is obtained with

$$\Gamma(N, E, \mu, \beta) = \frac{\sum_{i=1}^{R} f_i(N, E) \exp(-\beta E + \beta\mu N)}{\sum_{i=1}^{R} K_i \exp(-\beta_i E + \beta_i \mu_i N - C_i)} \tag{14}$$

where K_i is the total number of observations for each run, and the constants C_i are obtained iteratively from the relationship

$$\exp(C_i) = \sum_E \sum_N \Gamma(N, E, \mu_i, \beta_i). \tag{15}$$

Once the above equations are run to convergence, the probability distribution in particle number can be obtained by summing Γ over the energies. Phase coexistence at any given temperature is obtained by requiring that the distribution with respect to density has two distinct peaks, of equal height. Figure 5 shows the coexistence curves obtained for the cases $\gamma_{\rm m} = 12, 9, 6$. Studying phase coexistence at lower values of $\gamma_{\rm m}$ is

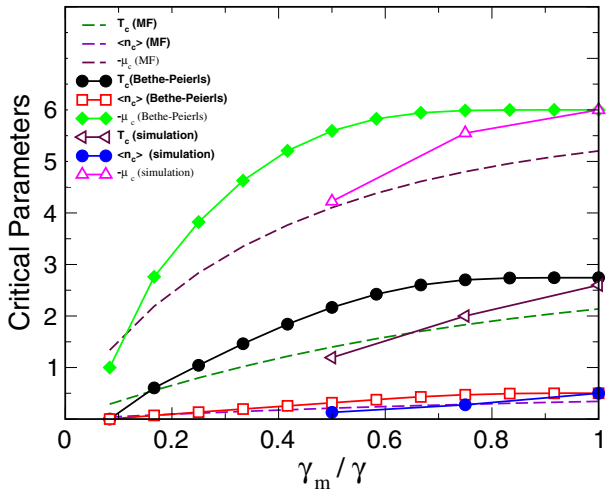

Figure 6. Comparison of the critical parameters from simulation with those of the mean field and Bethe–Peierls approximations, indicating that the critical parameters decrease more rapidly than suggested by the Bethe–Peierls approximation.

severely hampered by the extremely slow equilibration in the temperature range of interest and has not been attempted. In each of the cases studied, evaluating the coexisting phase densities is limited by the ability to resolve the coexisting density peaks, which is difficult as the critical point is approached. Nevertheless, it is clear from the data shown that the simulations confirm the trend seen in the calculations above, that the critical temperature and density decrease as γ_m decreases. Figure 6 shows the critical parameters in comparison with the mean field and Bethe–Peierls calculations. It is seen that the critical parameters drop more rapidly than suggested by the Bethe–Peierls calculations. The values of the critical parameters from the mean field calculation, surprisingly, compare somewhat better than the Bethe–Peierls calculations. Unlike the $\gamma_m = 12$ case, where the coexistence chemical potential and the mean of the coexisting densities are constant below the critical temperature, both these quantities increase as one moves to lower temperatures below the critical temperature.

In figure 7, we compare the spinodal locus from the mean field, Bethe–Peierls calculations with the coexistence line from simulations, for the case $\gamma_m = 6$. While the spinodal curve for the Bethe–Peierls calculation is nearly symmetric, we find that both the mean field and simulation results display a skew towards lower densities.

6. Conclusions

We have presented results for lattice gas models with the imposition of a constraint on the maximum number of bonds that particles can participate in. Mean field (Bragg–Williams and Bethe–Peierls) calculations and computer simulations using the histogram reweighting technique show that the critical temperature and density decrease as the maximum number of bonds allowed for a given particle is reduced. Also, we find that the density range of the coexistence region, where the liquid and gas phases coexist, shrinks

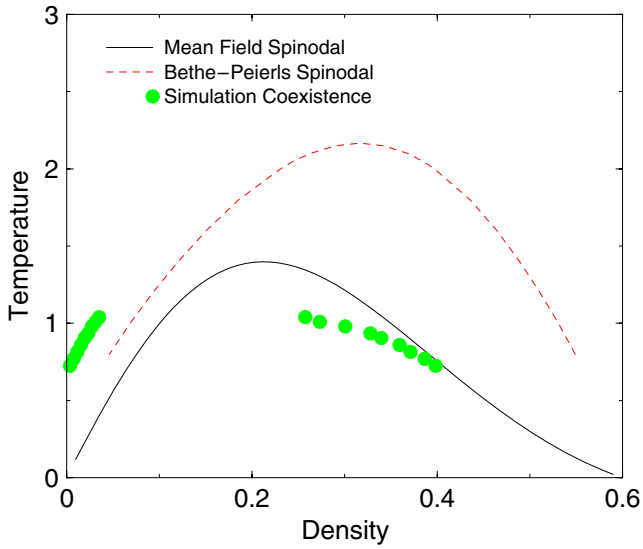

Figure 7. The coexistence curve for $\gamma_m = 6$ from simulations, compared with the spinodal curves from the mean field and Bethe–Peierls approximations.

as the maximum valency of the particles is reduced. These results are consistent with the results that have been obtained earlier for similarly defined continuum models [20, 21]. It is thus confirmed that valency reduction is effective in opening a large region of densities in which low temperature disordered states can be accessed in equilibrium. Studies of models with controlled valency, both on the lattice and off-lattice, may make it possible to disentangle gelation from phase separation.

Acknowledgments

FS and ELN acknowledge support from MIUR COFIN. SS acknowledges support from DST, India, and thanks the University of Roma 'La Sapienza' for hospitality.

References

[1] Verhaeg N A M, Asnaghi D and Lekkerkerker H, 1999 *Physica* A **264** 64
[2] Trappe V and Sandkühler P, 2004 *Curr. Opin. Colloid Interface Sci.* **8** 494
[3] Cipelletti L and Ramos L, 2004 *J. Phys.: Condens. Matter* **17** R253
[4] Sciortino F *et al*, 2005 *Comput. Phys. Commun.* **169** 166
[5] Rubinstein M and Dobrynin A V, 1999 *Curr. Opin. Colloid Interface Sci.* **4** 83
[6] Lomakin A, Asherie N and Benedek G B, 1999 *Proc. Nat. Acad. Sci.* **96** 9465
[7] Starr F W and Sciortino F, 2006 *J. Phys.: Condens. Matter* **18** L347
[8] Lodge J F M and Heyes D M, 1999 *Phys. Chem. Chem. Phys.* **1** 2119
[9] Bergenholtz J and Fuchs M, 1999 *Phys. Rev.* E **59** 5706
[10] Cates M E *et al*, 2004 *J. Phys.: Condens. Matter* **16** S4861
[11] Del Gado E, Fierro A, de Arcangelis L and Coniglio A, 2004 *Phys. Rev.* E **69** 051103
[12] Zaccarelli E, Sciortino F, Buldyrev S V and Tartaglia P, 2004 *Unifying Concepts in Granular Media and Glasses* ed A Coniglio, A Fierro, H J Herrmann and M Nicodemi (Amsterdam: Elsevier) p 181
[13] Sastry S, 2000 *Phys. Rev. Lett.* **85** 590
[14] Speedy R J, 2003 *J. Phys.: Condens. Matter* **15** S1243
[15] La Nave E, Mossa S, Sciortino F and Tartaglia P, 2004 *J. Chem. Phys.* **120** 6128
[16] Shell M S and Debenedetti P G, 2004 *Phys. Rev.* E **69** 051102
[17] Ashwin S S, Menon G I and Sastry S, 2006 *Europhys. Lett.* **75** 922

J. Stat. Mech. (2006) P12010

[18] Foffi G, De Michele C, Sciortino F and Tartaglia P, 2005 *J. Chem. Phys.* **122** 224903
[19] Manley S *et al*, 2005 *Phys. Rev. Lett.* **95** 23802
[20] Zaccarelli E *et al*, 2005 *Phys. Rev. Lett.* **94** 218301
[21] Bianchi E *et al*, 2006 *Phys. Rev. Lett.* **97** 168301
[22] Sear R P, 1999 *J. Chem. Phys.* **111** 4800
[23] Kern N and Frenkel D, 2003 *J. Chem. Phys.* **118** 9882
[24] Huang K, 2000 *Statistical Mechanics* (New York: Wiley)
[25] Ferrenberg A M and Swendsen R H, 1988 *Phys. Rev. Lett.* **61** 2635
[26] Ferrenberg A M and Swendsen R H, 1989 *Phys. Rev. Lett.* **63** 1195
[27] Panagiotopoulos A Z, Wong V and Floriano M A, 1998 *Macromolecules* **31** 912
[28] Panagiotopoulos A Z, 2000 *J. Phys.: Condens. Matter* **12** R25

J. Stat. Mech. (2006) P12010